


Design and optimization of a modified series hybrid electric vehicle powertrain

Proc IMechE Part D:
J Automobile Engineering
1–17
© IMechE 2018
Reprints and permissions:
sagepub.co.uk/journalsPermissions.nav
DOI: 10.1177/0954407018759357
journals.sagepub.com/home/pid


Swagata Borthakur and Shankar C Subramanian

Abstract

Hybrid electric vehicles are emerging technologies that are considered as eco-friendly alternative solutions to internal combustion engine-driven vehicles. This paper proposes a modified hybrid electric vehicle powertrain system that addresses the shortcomings of a series hybrid electric vehicle powertrain. The proposed configuration replaces the conventional generator of a series hybrid electric vehicle with an integrated starter generator that supports the traction motor of the vehicle during acceleration and peak torque requirements and maintains the state of charge of the batteries to provide an extended electric range of the vehicle. The work done in this paper can be categorized into two stages. The first stage is the methodical development of the powertrain in terms of initial parameter matching and sizing of the vehicle components by considering the fundamentals of longitudinal vehicle dynamics. The second stage describes the optimization of the proposed configuration to meet the design objective of maximizing fuel economy subjected to a set of vehicle performance constraints. The performance of the proposed powertrain was evaluated and compared with a series hybrid electric vehicle powertrain for an on-road Indian driving cycle using AVL CRUISE, which is a commercially available software for the study and analysis of road vehicle powertrains. Result analysis during initial parameterization showed a reduction in gross vehicle weight of the proposed configuration by 244 kg (1.5%) and an improvement in the average operating efficiency of the traction motor by around 11%, when compared to a series hybrid electric vehicle. Furthermore, the optimization results for the proposed configuration established an improvement in the fuel economy by 21% while meeting vehicle performance requirements.

Keywords

Hybrid electric vehicle powertrain, series hybrid electric vehicle, integrated starter generator, vehicle powertrain, component sizing, powertrain optimization

Date received: 1 May 2017; accepted: 12 January 2018

Introduction

In recent years, rapid urbanization and growth of motor vehicles have increased air pollution, health ailments, global warming, and instability of ecosystems. For emerging economies like India, economic development is accelerating the demand for transportation with energy consumption expected to increase by 70% in the next 10 years.¹ The transportation sector alone accounts for about one-third of the total crude oil consumption, which is widening the gap between domestic crude oil production and consumption. Most cities in India suffer extremely high levels of urban air pollution with the transportation sector being the major contributor to greenhouse gas (GHG) emissions. These concerns have accelerated the adoption of alternative solutions to reduce the dependency on fossil fuels for

transportation and developing new environmentally friendly vehicles.

Electric and hybrid electric vehicles (HEVs) have been recognized as promising technologies to replace the conventional internal combustion engine (ICE)-driven road vehicles, improving fuel economy and reducing harmful tail pipe emissions. The main hybrid electric powertrains available are series hybrid electric vehicles (SHEVs), parallel hybrid electric vehicles

Department of Engineering Design, Indian Institute of Technology Madras (IIT Madras), Chennai, India

Corresponding author:

Shankar C Subramanian, Department of Engineering Design, Indian Institute of Technology Madras (IIT Madras), Chennai 600036, India.
Email: shankarram@iitm.ac.in

(PHEVs), and series-parallel hybrid electric vehicles (SPHEVs).² SHEVs are suitable for heavy-duty commercial road vehicles including buses, trucks, and military vehicles, since they are capable of carrying the large payload of batteries and the electric propulsion system, along with their simple structure and control, lower emission, and higher amount of regenerative braking.³ SHEV configuration was also studied by researchers for sports cars and mid-size vehicles to overcome the challenge of limited space allocation by minimizing the size of the energy storage system (ESS) as well as maximizing fuel economy.^{4,5} In an SHEV, the electric motor, being the only source of propulsion, provides power to turn the wheels of the vehicle and recharge the batteries. The characteristic of the electric motor enables it to provide maximum torque in its low-speed region (up to its base speed), after which it enters the constant power region. SHEVs can be run in pure electric mode with zero emission, where the engine is not mechanically connected to the transmission, thereby ensuring that the engine is running only in its efficient regions (Figure 1).⁶ The main challenge, however, in designing an SHEV is the selection of the motor drive with proper power rating to meet vehicle performance requirements. Although single shaft PHEVs and plug-in HEVs have been studied in the areas of hybrid electric buses for city driving conditions,^{7,8} the use of SHEV configuration is justified in a city drive cycle where the electric motor provides the initial high torque requirement, thereby making the vehicle run almost in pure electric mode. This paper focuses on the study and analysis of the SHEV and the modified powertrain for a city bus under an urban start-stop driving condition.

Since an SHEV is an electric-intensive configuration, with the electric motor being the only traction source, the motor power rating and efficiency have a significant contribution to the overall vehicle performance and efficiency. Studies showed that the power rating of the electric motor during acceleration and grade climbing could be reduced to a minimum if the machine is operated mostly in its constant power region.⁶ As an SHEV is dependent purely on the traction motor for both steady state and dynamic load conditions, the motor operating points tend to spread extensively across its entire operating range, which makes the vehicle driving points at speeds and loads below the most efficient operating points of the electric motor.^{6,9} Various researchers have studied performance evaluation and efficiency of the electric machines in electric vehicles (EVs) and HEVs. Miller et al.¹⁰ showed that the improvement in the performance of the electric machine could be done either by incorporating a two-speed transmission system (also termed as two-speed EV drive) instead of a single gear box or by using a combination of two electric motors to adjust the motors' speeds for greatest tractive effort and for highest overall efficiency. A comparative analysis showed

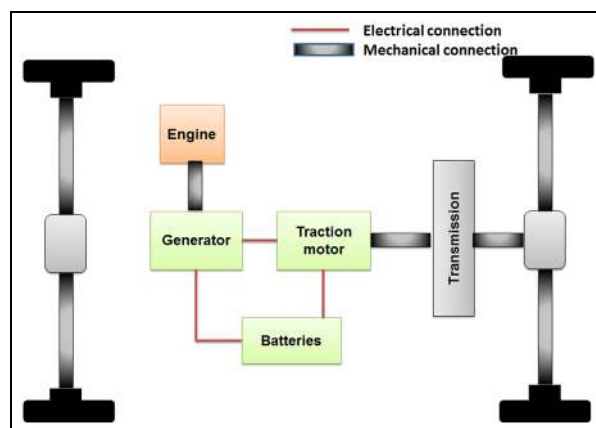


Figure 1. Layout of a rear wheel drive SHEV.
SHEV: series hybrid electric vehicle.

an improvement in motor operating regions when two equivalent traction motors were used instead of one large traction motor during pure electric drive.⁴ Zhu et al.¹¹ also developed an EV by replacing the single traction motor with two smaller motors driving two separate reduction gears, where the motors worked in parallel to provide power to the wheels. The use of two motors improved the motors' efficiency by around 7% and the electric range by 8%. The use of two traction motors instead of one was justified during high torque requirement, ensuring their optimized performance. Although a typical SHEV consists of two electric machines, namely, a generator and a traction motor, it is only the traction motor that provides the necessary torque to run the vehicle, while the generator combined with engine is used to maintain the state of charge (SOC) of the batteries. Thus, the generator in this case remains unused during pure electric driving, which accounts for almost two-thirds of total urban driving.¹² Hence, this paper investigates the vehicle performance by replacing the conventional generator of an SHEV with an integrated starter generator (ISG) to aid the main traction motor for propulsion during pure electric drive.

ISGs are one of the evolving technologies that are used in HEVs to achieve high peak power in a very short period of time.¹³ They are high torque density and efficient motors that provide extra drive force during additional torque requirement, work as a generator to recover electrical energy, and also as a starter motor to enable the start-stop function of the engine.^{13,14} The incorporation of ISGs has been mostly limited to mild HEVs having a parallel configuration.¹² Studies conducted on the use of an ISG in a pre-transmission PHEV showed an improvement in the overall efficiency by 20–30%.¹⁴ Zhou et al.¹⁵ developed a single-axle PHEV where the ISG is mounted directly on the engine crankshaft output, replacing the flywheel and separate starter and generator. These authors concluded that as compared to the traditional PHEV, the single-axle

PHEV improved acceleration performance by 9% and a reduction in fuel consumption by 18%. Fukuo et al.¹⁶ described the development of Honda Insight, which is an integrated motor assist (IMA) parallel hybrid configuration, with the motor assisting the engine during peak torque requirements and capturing regenerative energy during braking. Honda Insight was able to achieve low fuel consumption, low exhaust emission, and reduced gross vehicle weight (GVW). Thus, the incorporation of an ISG was able to improve the overall performance of PHEV as compared to its traditional counterpart. However, the use of an ISG and its effects are yet to be explored for an SHEV powertrain.

Motivated by these factors, this paper proposes a modified SHEV powertrain by replacing the generator with an ISG, that works both as a generator to convert engine power into electricity to charge the batteries and as a motor to drive the wheels, thereby assisting the main traction motor during pure electric driving. Thus, the torque requirement by the vehicle is distributed between the two electric machines during pure electric driving, which would operate the motors in their most efficient regions, thereby increasing the overall efficiency of the powertrain. The objective of this research work is to analyze the performance of the proposed powertrain configuration in terms of electric motors' efficiency and vehicle fuel economy, for urban/city driving with frequent start-stop conditions, by considering an on-road Indian drive cycle (IDC), where the vehicle runs in pure electric mode with both the ISG and the traction motor powering it.

This study proposed and analyzed a modified SHEV powertrain by replacing the conventional generator with an ISG, that works both as a generator to convert engine power into electricity to charge the batteries and as a motor to drive the wheels, thereby assisting the main traction motor during pure electric driving.

The design of a vehicle powertrain starts with initial parameter matching and sizing of its components, which should satisfy the following vehicle performance constraints:¹⁷ (1) initial acceleration, (2) gradeability, and (3) maximum cruising speed. The next step involves the development of the control strategy for the vehicle powertrain to control the operation and power flow based on the driver's command through accelerator and brake pedals. An on-road IDC was considered to evaluate the developed powertrain and analyze the results.

The completion of the initial parametric design was followed by the optimization of the vehicle powertrain for better vehicle performance and improved fuel efficiency. Various optimization algorithms (both gradient based and derivative-free^{18,19}) can be found in the literature. The benefit of derivative-free algorithms such as divided rectangles (DIRECT) and genetic algorithm (GA)¹⁸ is that the objective functions do not rely on derivatives. Moreover, DIRECT is a deterministic global optimization algorithm, which ensures that the objective function converges in a finite time interval.

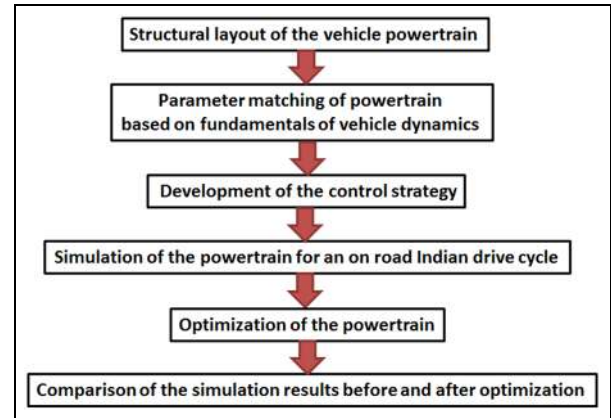


Figure 2. Methodology adopted for the development of HEV configurations.

HEV: hybrid electric vehicle.

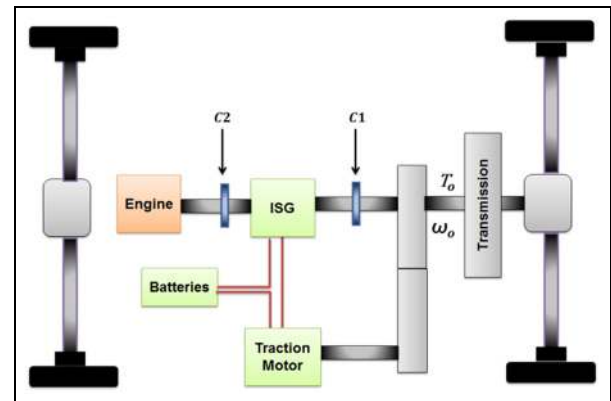


Figure 3. Layout of the proposed configuration.

For the optimization of the proposed configuration, DIRECT algorithm was used in this study.

This paper starts with initial parameter matching of the proposed configuration and an SHEV given a set of vehicle performance requirements. Completion of the initial parameter matching is accompanied by development of the control strategy for the proposed configuration. The final stage involves the optimization of the proposed configuration followed by comparative analysis before and after optimization.

In summary, the work presented in this paper can be visualized as given in Figure 2.

Design of the proposed configuration

The proposed powertrain consists of a downsized ICE, a traction motor, an ISG, an energy storage device (batteries), and a mechanical coupler. The powertrain configuration layout is shown in Figure 3, in which the ISG and traction motor output shafts are mechanically coupled by a coupler to add the torque output from both these power sources. The output power from the coupler is then transmitted to the wheels through the

Table 1. Comparison between SHEV and the proposed configuration.

| SHEV | Proposed configuration |
|--|--|
| Downsized engine operating at its efficient region. A large traction motor that provides torque to propel the vehicle. A generator that runs along with the engine to generate electric energy to charge the batteries and/or power the motor. | Downsized engine operating at its efficient region. A downsized traction motor that provides torque to propel the vehicle. An ISG that works as a motor to support the traction motor during peak torque requirements and as a generator that runs along with the engine to generate electric energy to charge the batteries and/or power the motor. |
| No separate clutch arrangement. | Two clutch arrangement for independent operation of the ISG as a motor and as a generator. |
| Single speed gear box. | A single speed gear box and an additional torque coupler that couples the torque outputs from ISG and traction motor during motoring mode. |

SHEV: series hybrid electric vehicles; ISG: integrated starter generator.

transmission. The engine is mechanically disconnected from the transmission system; hence, its operation is independent of the vehicle load conditions.

A brief comparison of the components between the SHEV and the proposed configuration is summarized in Table 1.

The incorporation of the ISG instead of a conventional generator provides the following benefits:

- ISG can work as a starter motor to start the engine, thereby eliminating the need of a separate starter motor.
- It works as a generator to be run along with the engine either to charge the battery or power the traction motor.
- It works as an electric motor to assist the main traction motor for propelling the vehicle during high torque requirements. In an electric drive, the power demand from the vehicle can be distributed between the ISG and the traction motor with proper power ratings.
- Since the ISG assists the vehicle for propulsion, the traction motor can be downsized appropriately based on the vehicle performance requirements. Since during city driving, the oversized traction motor of an SHEV runs in part load conditions, the downsizing of the traction motor in the proposed configuration will help the motor to run mostly in full load conditions with the ISG providing the extra power demand. Hence, the overall electrical efficiency of the motors can be increased.

Clutches C1 and C2 (Figure 3) are incorporated to enable the independent operation of ISG as a generator and an assisted motor. When the ISG works in motoring mode, C1 is closed to connect the ISG to the torque coupler and support the traction motor to provide the necessary torque to the vehicle. C2 remains open at this time. When the ISG works in generating mode, C1 is opened so that it is disconnected from the torque coupler, while C2 is closed. The ISG and the engine work

Table 2. Vehicle parameters.

| Parameters | Values |
|----------------|---------------------|
| Glider mass | 3940 kg |
| Cargo mass | 9700 kg |
| ICE power/mass | 200 kW/545 kg |
| GVW | 14,351 kg |
| C_d | 0.440 |
| A_f | 6.50 m ² |
| f_r | 0.009 |
| r | 0.50 m |
| L | 4.75 m |

ICE: internal combustion engine; GVW: gross vehicle weight.

together to generate the necessary electric energy to charge the batteries. Hence at a time, the ISG can operate either as a generator or as a motor. Only one clutch can be engaged at a time for the power flow from the source to the wheels. If both clutches are closed at the same time, the electric machine has to operate both as a motor and as a generator at the same time, which is not practically feasible. Also, parallel operation of the vehicle is not possible, since the engine is not mechanically connected to the transmission. The proposed configuration is a modification of an SHEV, where the generator of a typical SHEV is replaced by an ISG so that it can behave both as a motor and as a generator.

The working mode of the ISG is controlled by the control strategy that is explained in the subsequent sections.

Vehicle parameters and specifications

To study and design the HEV powertrain, a heavy duty truck²¹ was considered in this study. The vehicle parameters and drive specifications are given in Tables 2 and 3, respectively. These data were used in the design of the powertrain components and simulation.

The design of the powertrain in this section involves estimating the power specifications of ICE, traction motor, ISG, transmission, and batteries to meet the

Table 3. Vehicle performance specifications.

| Specifications | Values |
|-----------------------------|----------------|
| Maximum speed (v_{max}) | 95 km/h |
| Gradeability | 15% at 16 km/h |
| Acceleration speed | 0–50 km/h |
| Acceleration time | 13 s |
| Pure electric range | 100 km |

drive specifications. The control strategy on torque distribution between ISG and traction motor is discussed in the subsequent section.

As the vehicle is modified from a conventional to an HEV, various components are added to the base vehicle such as a downsized ICE, electric machines, batteries, and transmission system. For better comparison, the total mass of the vehicle (also known as GVW) is split in terms of body mass, chassis mass, powertrain mass, and cargo mass. The body mass and the chassis mass (together termed as the glider mass) and the cargo mass for the hybrid and conventional vehicles are considered identical in this study. The powertrain mass changes depending on the powertrain used. So the GVW can be written as follows

$$m_{tot} = m_{glider} + m_{cargo} + m_{powertrain} \quad (1)$$

The objective here is to minimize the GVW of the proposed configuration while satisfying the vehicle requirements. This is done by studying the characteristics of the powertrain components. Parameter matching of each of the powertrain components is discussed below.

Equations governing the vehicle drive performance

The basic equation governing the longitudinal motion during acceleration can be written as follows

$$F(t) = \frac{Wa}{g} = F_t(t) - (R_a(t) + R_f(t) + R_g(t)) \quad (2)$$

The vehicle performance requirements are typically described by its maximum speed, acceleration, and gradeability.² The maximum vehicle speed is limited by the maximum speed of the output shaft of the mechanical coupler (Figure 3) that is given as follows

$$v_{max} = \frac{\pi \omega_{o, max} r}{30 i_g (1 - s)}$$

where

$$i_g = i_o i_{fd} \quad (3)$$

The power output to achieve this maximum speed is given as follows

$$P_{max}(t) = \frac{1}{\eta_t} \left(Mgf_r + \frac{1}{2} \rho C_d A_f v_{max}^2 \right) v_{max} \quad (4)$$

Similarly, the power required to achieve a grade θ_s is given as follows

$$P_{grade}(t) = \frac{1}{\eta_t} \left(Mgf_r \cos \theta_s + \frac{1}{2} \rho C_d A_f v_{grade}^2 + Mg \sin \theta_s \right) v_{grade} \quad (5)$$

The acceleration performance is evaluated by the time required by the vehicle to accelerate from rest to a certain longitudinal speed (v_{rv}). The power required for acceleration is provided by the electric machines which can be written as⁶

$$P_{acc}(t) = \frac{1}{\eta_t} \left(\frac{\gamma M}{2 I_f} (v_{rm}^2 + v_{rv}^2) + \frac{2}{3} Mgf_r v_{rv} + \frac{1}{5} \rho C_d A_f v_{rv}^3 \right) \quad (6)$$

ICE

The engine/generator is used to supply the steady-state power to prevent the batteries from being discharged completely.² Two driving conditions need to be considered:

- Driving at a constant speed on a highway, where the engine/generator should be able to produce sufficient power to support the vehicle speed.
- Frequent stop-and-go pattern, where the engine/generator should produce sufficient power to maintain the SOC of the batteries at a certain level to support vehicle acceleration and grade climbing.

At a constant speed v , on a flat road, the continuous power requirement is given by

$$P_{eng}(t) = \frac{1}{\eta_t \eta_g} \left(Mgf_r + \frac{1}{2} \rho C_d A_f v^2 \right) v \quad (7)$$

The engine power rating for the vehicle driving at a constant speed of 60 km/h on a flat highway was calculated using equation (7) to be 48 kW. The engine model was taken from ADVISOR²⁰ by selecting (Caterpillar 312 6E) 7 L CI engine weighing 303 kg. A generator efficiency of 90%²⁰ was considered.

Electric machines

During electric drive, the output power of both the traction motor and ISG (working as a motor) are combined together by a mechanical coupling as shown in Figure 3. Mechanical couplings are broadly classified as torque coupling and speed coupling.² In torque coupling, the torques of both the power sources are controlled independently and added together, but their speeds are dependent on each other. In speed coupling, the speeds of the power sources are controlled independently and added, with their torques linked and dependent on each other. Since

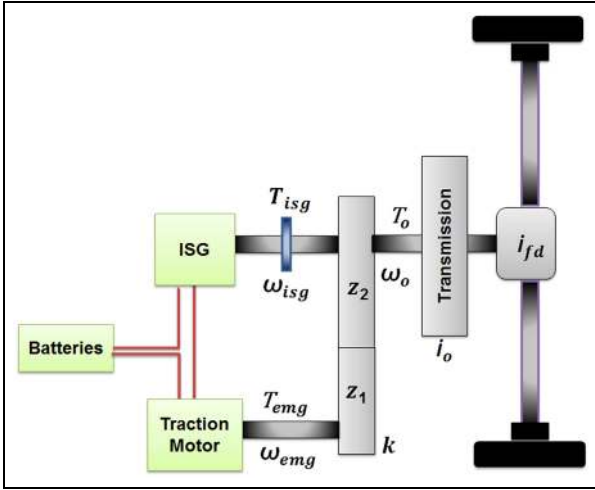


Figure 4. Torque distribution in the proposed configuration.

this paper focused on the distribution of torque between the ISG and the traction motor during peak torque requirements, a torque coupler was used to analyze the performance of the hybrid powertrain. Two clutches were incorporated for the independent working of the ISG as a motor and a generator.

The torque coupler is designed such that the electric machines' characteristics meet the vehicle performance. Figure 4 shows the torque coupling where the ISG power is directly transmitted to the transmission system, whereas the traction motor power is transmitted through a geared pair. The output torque from the ISG and traction motor reaching the wheels is magnified by the transmission system.

The ISG speed and torque are directly transmitted to the transmission, whereas the traction motor speed and torque are varied by the torque coupler with a ratio k , given as $k = (z_1/z_2)$, where z_1 is the number of teeth on the input shaft and z_2 are the number of teeth on the output shaft of the torque coupler geared wheel.

The speed of the ISG, the traction motor, and the output shaft are related to the torque coupler ratio k as given by equations (8) and (9)

$$\omega_{o, \max} = \frac{\omega_{emg, \max}}{k} \quad (8)$$

$$\omega_o = \omega_{isg} = \frac{\omega_{emg}}{k} \quad (9)$$

The maximum speed of the electric machines limits the sizing of the transmission and the torque coupler gear ratio. The control strategy is developed such that the maximum speed of the vehicle is provided by the traction motor.

The torque requirement for gradeability is given as follows

$$T_{grade}(t) = \frac{(Mgf_r + \frac{1}{2}\rho C_d A_f v_{grade}^2 + Mg \sin \theta_s)r}{i_g \eta_t} \quad (10)$$

and this is distributed between the ISG and the traction motor.

The electric machines are the torque providers during both climbing a grade and acceleration. To compute the power requirement during acceleration, the characteristics of the electric machines in extended-speed range need to be studied. Ehsani et al.⁶ studied the motor characteristics in the extended-speed constant power region and found out that initial acceleration and grade conditions could be met with minimum power rating if the powertrain can be operated mostly in constant power region. But increasing the extended-speed region increases the torque rating of the motor, which in turn increases the motor weight. So the characteristics of the electric machines affect the GVW. The power required for acceleration can be written in terms of speed ratio $x = (\text{maximum speed}/\text{base speed})^{21}$ as follows

$$P_{acc} = \frac{1}{\eta_t} \left(\frac{\gamma M}{2t_f} v_{rv}^2 \left(1 + \frac{1}{x^2} \frac{v_{\max}^2}{v_{rv}^2} \right) + \frac{2}{3} Mgf_r v_{rv} + \frac{1}{5} \rho C_d A_f v_{rv}^3 \right) \quad (11)$$

Since the development of an ISG is beyond the scope of this paper, hence, based on the literature survey, three different ISGs with high torque density were considered with speed ranging from 3000 to 5000 r/min.^{22–24} The following generalizations have been made for the parameter matching of the electric machines:

- Variation of acceleration power and torque with respect to extending the constant speed range is considered the same for both the ISG and the traction motor.
- As established by Hughes and Drury,²⁵ the relationship between motor torque and its volume is given as follows

$$T \propto \bar{B} \bar{A} \bar{D}^2 L$$

During the simulation study, for a given specific machine, the overall volume of the motor was assumed to be directly proportional to the torque it produces. The masses of the specific motors at different base speeds were calculated assuming the motor mass to be proportional to the peak motor torque.

At higher vehicle speeds, the load requirement to maintain the vehicle speed decreases,²⁶ whereas the electrical power consumed by a high-speed motor at low load is high. Since for the proposed configuration, the torque coupler provides an additional torque coupling with speeds constrained by equation (9), medium speed induction motors ranging from 7000 to 10,000 r/min²⁷ were used as traction motors for simulation.

The power curve required for acceleration was obtained from equation (11) through numerical simulation for speed ratios varying from 2 to 5. The

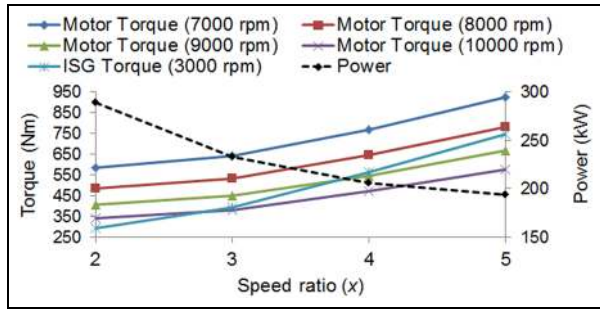


Figure 5. Variation of acceleration power and machines torques with x for 3000 r/min ISG and four medium speed motors. ISG: integrated starter generator.

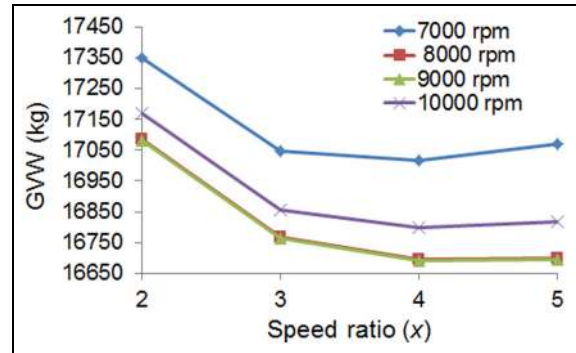


Figure 6. Variation of GVW with x for 3000 r/min ISG and four medium speed motors. GVW: gross vehicle weight; ISG: integrated starter generator.

corresponding torque output was simultaneously calculated for four medium speed traction motors (with speed ranging from 7000 to 10,000 r/min) and three ISGs of 3000, 4000, and 5000 r/min, respectively. The variation of power required for acceleration and the electric machine torques with speed ratio is represented graphically in Figure 5 for the four traction motors and 3000 r/min ISG.

From Figure 5, it was observed that increasing the speed ratio decreases the power required for acceleration. Since the motor input power is provided solely by the battery pack, hence, a reduction in power demand decreases the number of battery cells. However, increasing the speed ratio increases the motor torque almost in a linear fashion, which increases the motor weight and in turn the vehicle weight. If the decrease in weight of the battery pack is more than the increase in weight of the electric machines, then the overall weight of the vehicle would decrease. An iterative simulation was done to find the parameters of the electric machines and the battery pack by determining the proper value of speed ratio to minimize the GVW.

Figures 6–8 show the effect of GVW of the vehicle with respect to x for four traction motors while considering three ISGs with speeds of 3000, 4000, and 5000 r/min, respectively.

It can be observed from Figures 6–8 that, as the speed ratio increased, the torque rating of the motors also increased making them bulkier. However, because the power ratings of the motors decreased at the same time, the size of the battery pack providing power to the motors reduced. The GVW first decreased to a certain value after which it increased. This happened because the decrease in battery weight dominated the increase in the motors weight at first. But after a certain value of x , the increase in motor weight was more than the decrease in the battery weight, leading to an overall increase in the GVW.

From the above analysis, the traction motor with the maximum speed of 9000 r/min gave the lowest GVW of 16,657 kg at $x = 4$ with a peak torque of 508 Nm and

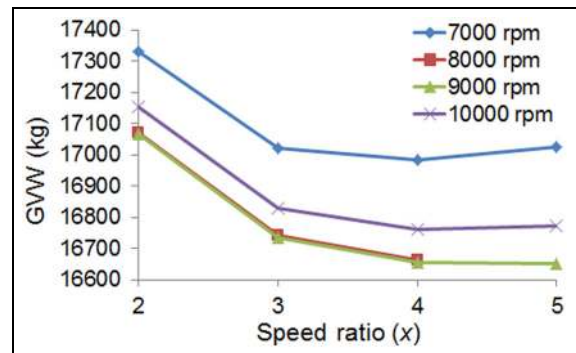


Figure 7. Variation of GVW with x for 4000 r/min ISG and four medium speed motors. GVW: gross vehicle weight; ISG: integrated starter generator.

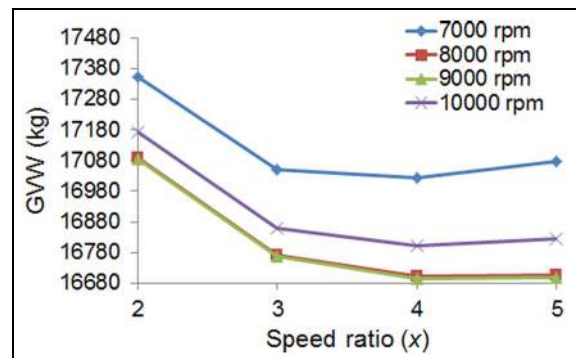


Figure 8. Variation of GVW with x for 5000 r/min ISG and four medium speed motors. GVW: gross vehicle weight; ISG: integrated starter generator.

a power rating of 135 kW. It satisfied both the acceleration performance and the maximum torque required for gradeability. A 350-V peak voltage motor was considered in this study. The ISG with speed range of 4000 r/min was chosen providing a peak motor torque of 330 Nm and a power rating of 54 kW. During initial parameter matching, the electric machines' efficiencies were

assumed constant for both the proposed configuration and the SHEV. However, during subsequent analysis with AVL CRUISE, their efficiency maps were used to better reflect real operating conditions.

Transmission

A single gear transmission, being simple without the need of a separate control module, was used in this study. As maximum speed of the vehicle is provided by the traction motor, from equation (3), the transmission ratio, i_{gs} , was calculated to be 7.13. As described in the previous section, the speed of the ISG, traction motor, and the output shaft are related to the torque coupler ratio (equation (9)). Based on the selection of the traction motor and the ISG, the ratio of torque coupler, k , was fixed to be 2.25, which also satisfies the torque requirement for gradeability as given by

$$T_{grade}(t) \leq T_{isg} + kT_{emg} \quad (12)$$

Battery pack

The size of the battery pack is dependent on the electric machine's peak power. During acceleration and cruising, the battery power that is delivered to the motor is given as follows

$$P_b = \frac{P_m}{\eta_m \eta_{bd}} + \frac{P_{isg}}{\eta_{isg} \eta_{bd}} \quad (13)$$

Depending on the capacity of the battery, the battery energy (in kW h) can be calculated as follows

$$E_b = \frac{V_b C}{1000} \quad (14)$$

Lithium ion (Li-ion) batteries were considered for this study providing an energy output of 150 kW h with 90% efficiency.²¹ The details of these specifications can be found in Borthakur and Subramanian.²¹ During initial parameter matching, the battery efficiency was assumed to be this same constant value for both the proposed configuration and the SHEV. However, during subsequent analysis with AVL CRUISE, the efficiency maps provided by AVL CRUISE were used to better reflect real operating conditions. The battery pack has an initial capacity of 70 Ah and the SOC variation was taken between 0.45 and 0.8.

Control strategy

A control strategy commands the operation of each component of a vehicle. The vehicle controller receives operation commands as signals from acceleration pedal/brake pedal, vehicle speed, and the powertrain components and then decides on the use of the appropriate operation modes. Development of a control strategy depends on the topology of the vehicle powertrain and they are different for different configurations.

Based on the proposed configuration, a new rule-based control strategy was developed in this paper for proper operation of the vehicle. The main operating modes of the powertrain can be divided as follows: pure electric mode, extended range mode, and regenerative braking mode. The pure electric mode can have a single-motor drive or a dual-motor drive depending on the torque requirement from the vehicle. The extended range mode is the hybrid electric mode, in which the engine-generator either charges the batteries or provides electric power to the traction motor to maintain the vehicle performance.

The flowchart describing the control logic used in this paper is shown in Figure 9. The operating modes and the working conditions of the powertrain along with the state of clutch 1 (C1) and clutch 2 (C2) used in this paper are tabulated in Table 4.

Design of the SHEV configuration

To provide a comparative analysis between the proposed configuration and an SHEV powertrain, initial parameter matching of SHEV was carried out by taking the same conventional vehicle as the base vehicle. The characteristics of different components were studied to minimize the GVW of the powertrain. Component sizing of the SHEV is summarized below.

Engine-generator

In an SHEV, the engine produces necessary energy for motion of the vehicle such that it can directly power the traction motor when the battery SOC is low.² The engine power rating for the vehicle driven on a flat highway was calculated using equation (7) and found out to be 50 kW.

Electric motor

The traction motor is connected to the wheels through a single-step gear box and final drive. As it is the only torque provider to the wheels, proper power rating of the traction motor becomes very important. Four different motors with maximum speeds ranging from 9000 to 12,000 r/min²⁴ were used to study the effect of extending the constant power region on the motor ratings. An iterative simulation was done to find the motor and batteries masses, thereby calculating the parameters of the traction motor and the batteries. Figure 10 shows the torque rating with respect to speed ratio x , while Figure 11 shows the effect of GVW of the vehicle with respect to x for four different motors with speed ranging from 9000 to 12,000 r/min. Same trend as followed by the proposed configuration could be found out here for variation of motor torque and GVW with respect to x .

From the graph, it was found out that the motor with maximum speed of 12,000 r/min gives the lowest GVW of 16,901 kg at $x = 5$ with a peak torque of 729.40 N m and a power rating of 200 kW, satisfying

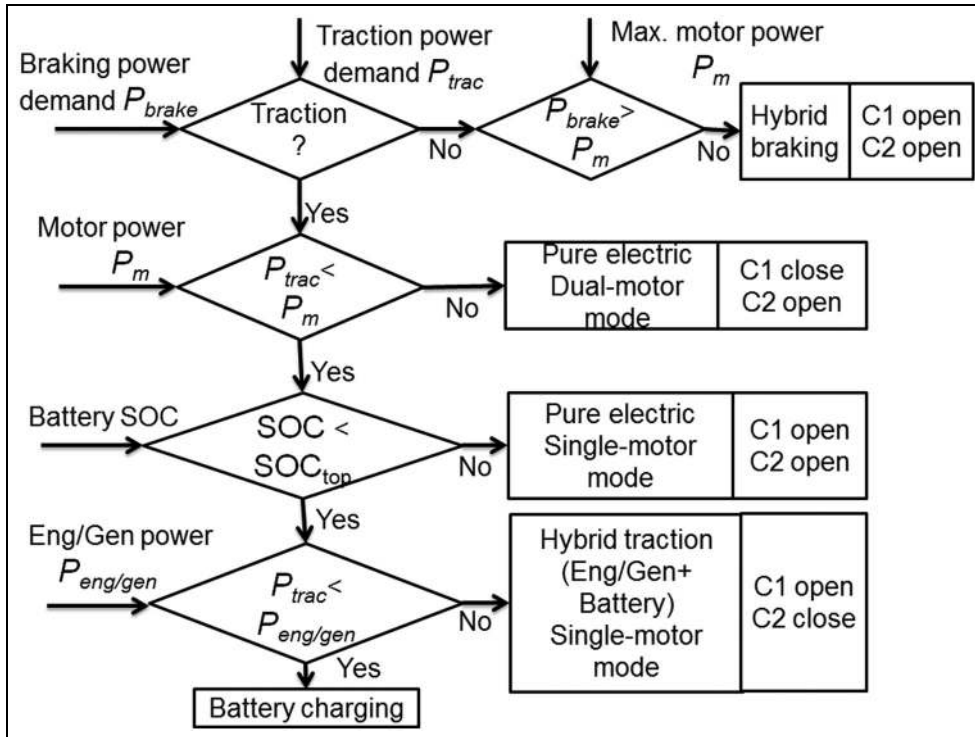


Figure 9. Flowchart describing the control logic.

Table 4. Operating modes of the proposed configuration.

| Operating modes | Remarks | Working conditions of electric machines | Engine | Batteries | State of clutches |
|------------------|--|--|----------------------|---|----------------------|
| Pure electric | When load torque T_L is less than the torque output of traction motor T_L is greater than the torque output of traction motor | Single-motor drive Traction motor: On. Drive the wheels ISG: Off | Off | Discharge energy to traction motor | C1 open C2 open |
| | | Dual-motor drive Traction motor: On. Drive the wheels ISG: On (motor mode). Drive the wheels | Off | Discharge energy to traction motor and ISG | C1 closed C2 open |
| Extended range | When the load power P_L is less than the motor power and the SOC is low | Traction motor: On. Drive the wheels ISG: On (generator mode) | Charge the batteries | Get energy from engine-generator | C2 closed C1 open |
| Braking/downhill | Regenerative braking | Traction motor: On (generator mode) ISG: Off | Off | Get charge energy from regenerative braking | C1 open C2 open |
| | Vehicle stop with low SOC | Traction motor: Off ISG: On (generator mode) | Charge the batteries | Get charge energy from engine-generator | C1 open C2 closed |

ISG: integrated starter generator; SOC: state of charge.

both the acceleration performance and maximum torque required for gradeability.

providing an output power of 234 kW with 90% efficiency and energy output of 162 kWh.

Battery pack

The battery power should be able to deliver the motor peak power. The battery energy was calculated using equation (14). The battery pack of Li-ion was used

Transmission

The gear ratio was designed in such a way that the vehicle reaches its maximum speed at the maximum speed of the motor (equation (3)). Since the torque-speed

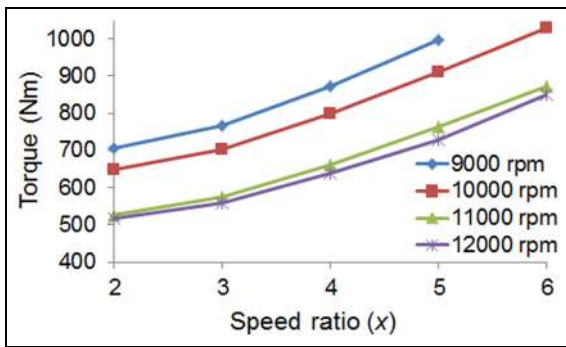


Figure 10. Torque output of motor with x .

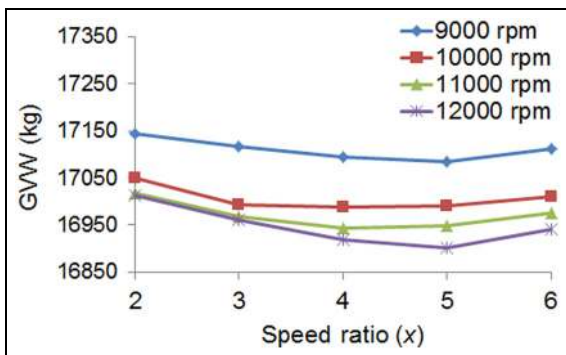


Figure 11. Variation of GVW with x .
GVW: gross vehicle weight.

characteristic curve of an electric motor is much closer to the ideal, a transmission ratio of 20.81 was calculated for the SHEV with a motor maximum speed of 12,000 r/min.

Control strategy

Most commonly used control strategies available in the literature are as follows: (1) maximum SOC of peak power source (PPS) and (2) engine turn-on and turn-off (engine on-off) or thermostat strategy.⁶ The main emphasis of the maximum SOC of PPS control strategy is to maintain the SOC of the battery at high level. But it does not guarantee the engine/generator to always operate at its optimum level.⁶ This may compromise the efficiency of the drive train. Hence, in this study, the thermostat control strategy was used where the operation of engine/generator is controlled solely by the SOC of the batteries.⁶

Optimization of the proposed configuration

After initial parameter matching and component sizing, optimization of the vehicle powertrain is the next step to achieve better vehicle performance and fuel economy. The optimization of the vehicle component parameters was conducted by the combined simulation of MATLAB/SIMULINK and AVL CRUISE. The

Table 5. Design variables used.

| Design variables | Nomenclature | Lower bound | Upper bound |
|-------------------------|---------------|-------------|-------------|
| ICE power scale | fc_pwr_scale | 1 | 3 |
| Motor torque scale | mc_trq_scale | 0.8 | 3 |
| ISG torque scale | isg_trq_scale | 0.8 | 3 |
| Number of battery cells | ess_num | 120 | 200 |
| Battery capacity (Ah) | ess_cap_scale | 8 | 20 |

ICE: internal combustion engine; ISG: integrated starter generator.

optimization algorithm was programmed in MATLAB, while the simulation calculation for the vehicle performance was done in CRUISE.

Optimization algorithm

Based on the literature survey, DIRECT algorithm (Jones, 2001) was chosen for this research work, as it is a deterministic global optimization algorithm that does not rely on derivatives and ensures that the objective function converges to a global optimum in finite time.

Optimization function

The objective considered for component size optimization was to maximize the fuel economy by minimizing the fuel consumption for an on-road IDC. The fuel consumption for electric and hybrid vehicles was calculated in terms of miles per gallon gasoline equivalent (mpgge).

Design variables and constraints

The design variables considered for optimization are engine power, motor power, ISG power, battery cells, and battery capacity. The constraint conditions were indicators of the dynamic performance that need to be fulfilled by the vehicle. The constraint conditions used for the optimization are as follows:

1. *Acceleration performance.* Time required by the vehicle to accelerate from 0 to 50 km/h.
2. *Grade.* Gradeability achieved by the vehicle at 16 km/h.
3. Difference between the drive cycles requested speed and the actual vehicle speed at every second during the drive cycle.
4. Difference between the initial and final SOC of the batteries.

The design variables were defined in terms of scaling factors, which when multiplied by the original values gives the actual values of the variables after optimization. The selected design variables are listed in Table 5. The constraint conditions in terms of vehicle performance used for optimization are given in Table 6.

Table 6. Constraint conditions.

| Constraints | Description | Requirements |
|-------------|--|----------------------|
| accel_time | Acceleration of 0–50 km/h | ≤ 13 s |
| grade | Gradeability at 16 km/h | $\geq 16\%$ for 60 s |
| delta_trace | Difference between drive cycle requested speed and vehicle achieved speed at every second during the drive cycle | ≤ 3.2 km/h |
| Delta_soc | Difference between final and initial SOC | $\leq 0.5\%$ |

SOC: state of charge.

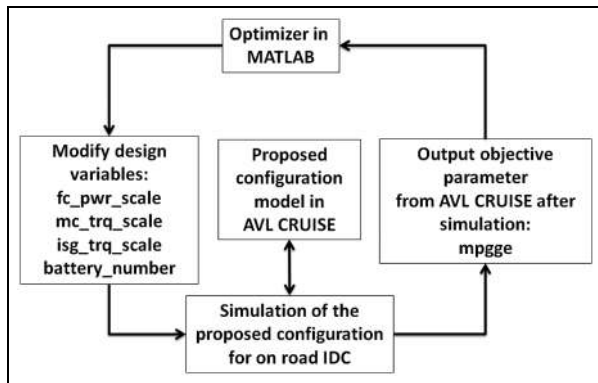


Figure 12. Flowchart of the optimization process.
IDC: Indian drive cycle.

Optimization procedure

The flowchart of the optimization procedure is shown in Figure 12. The optimizer was developed in MATLAB based on DIRECT algorithm, which was integrated with AVL CRUISE. The powertrain was simulated at first for an on-road IDC in AVL CRUISE using the initial values of the design variables to find the objective and constraint functions. These simulation results were imported into MATLAB to generate a new set of design variables using the optimization algorithm, that were returned to AVL CRUISE for the vehicle to be simulated again. The objective and constraint functions were calculated, with the variables restricted within their limits during the optimization process. The iterations continued until the convergence of the objective and the constraint functions was obtained. With this, the optimal objective value in terms of mpgge was achieved.

Simulation results and discussions

Analysis of the initial parameter matching of the HEV powertrains

Using the fundamentals of vehicle dynamics, initial parameter matching and component sizing of both the SHEV and the proposed configuration were

Table 7. Parameter matching comparison of the vehicles.

| Components | ICE-driven vehicle | SHEV | Proposed configuration |
|--------------|--------------------|---------------------------------------|-------------------------------------|
| Engine | 200 kW | 50 kW | 42 kW |
| Motor | – | 200 kW 12,000 r/min $T=729$ N m | 135 kW 9000 r/min $T=508$ N m |
| Generator | – | 55 kW 7000 r/min | – |
| ISG | – | – | 54 kW 4000 r/min $T=330$ N m |
| Transmission | 6 speed AMT | $i_g = 20.81$ | $i_g = 7.13$ $k = 2.25$ |
| Battery pack | – | 162 kW h $C = 72$ Ah | 150 kW h $C = 70$ Ah |
| GVW | 16,200 kg | 16,901 kg | 16,657 kg |

ICE: internal combustion engine; SHEV: series hybrid electric vehicle; GVW: gross vehicle weight.

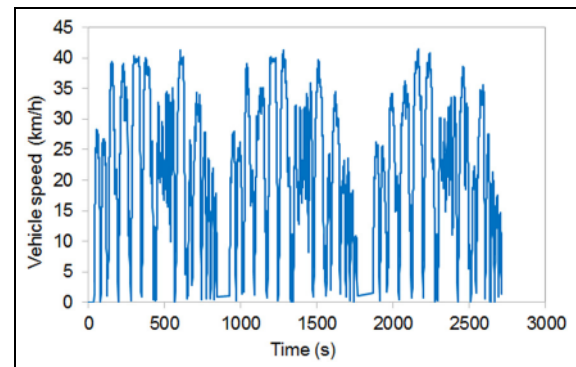


Figure 13. On-road measured Indian drive cycle.²⁸

accomplished. The parameter matching was done using an iterative simulation where the individual component masses were taken into account to calculate the GVW of the HEVs. Table 7 summarizes and compares the parameter matching of the proposed configuration and the SHEV with the conventional ICE-driven vehicle.

Comparison analysis of the initial parameterization (Table 7) showed a reduction of GVW of the proposed configuration by 244 kg (1.5%), as compared to SHEV. Downsizing of the ICE and the traction motor by 16% and 32.5%, respectively, could also be observed in the proposed configuration when compared to SHEV.

After the completion of initial parameter matching, simulation was carried out across an on-road IDC (Figure 13)²⁸ to evaluate and compare the performance of the proposed configuration with reference to the SHEV powertrain.

AVL CRUISE,²⁹ a software used for commercial road vehicle powertrain analysis, was used to simulate the HEV powertrains. The application programming interface (API) provided by AVL CRUISE was used to implement the control strategy in MATLAB/Simulink, while the SHEV and the proposed powertrain model

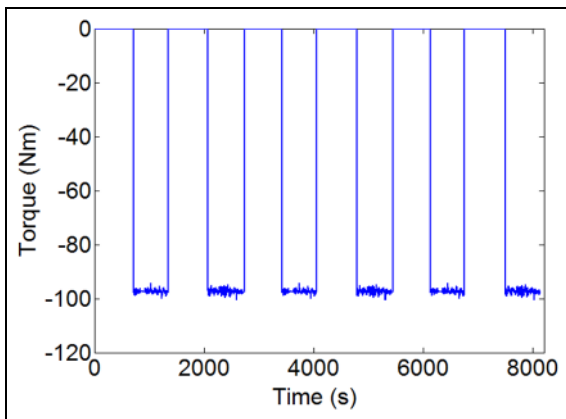


Figure 14. Output torque of the generator of SHEV. SHEV: series hybrid electric vehicle.

along with the simulation calculation for vehicle performance were done on CRUISE GUI. Information regarding the powertrain components and driver's demand were transferred via the API of AVL CRUISE to MATLAB/Simulink, where the signals were analyzed by the control strategy. The analyzed results from the control strategy were sent back to CRUISE via the interface, where the simulation outputs were obtained for both the powertrains.

SHEV configuration

Initial simulation of the SHEV using AVL cruise generated the torque output and efficiency of the traction motor across the on-road IDC, where the motor is the only torque provider for the powertrain. Figure 14 gives the torque output of the traction motor of the SHEV powertrain across the on-road IDC, where the motor is the only torque provider for the powertrain. The average efficiency of the motor across the on-road IDC repeated four times was calculated to be 70.93%. Figure 14 shows the working mode of the generator of the SHEV powertrain during low battery SOC, where the generator and the engine are switched on as they charge the batteries together. The efficiency of the electric machines was taken constant during initial parameter matching of the vehicle powertrain. However during simulation of the vehicle powertrain in AVL Cruise, its efficiency varied with the load torque to reflect the operating points of the motors.

Proposed configuration

Figure 15 shows the comparison of torque output of the traction motors of SHEV and the proposed configuration when simulated across the on-road IDC repeated four times, while Figure 16 shows the comparison of the efficiency of the traction motors of SHEV and the proposed configuration. Figure 17 shows torque output of the ISG for the same drive cycle. From Figure 17, it can be found out that ISG worked in

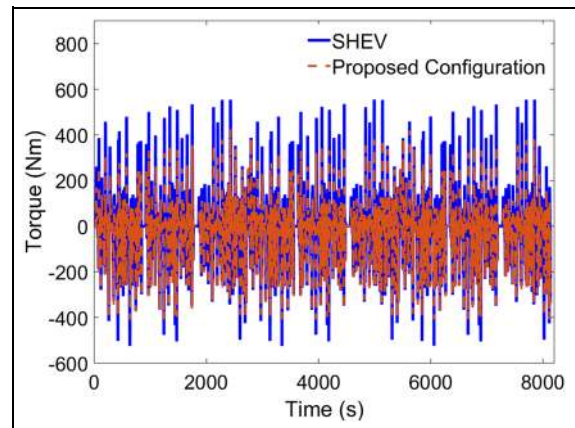


Figure 15. Comparison of traction motor torque for SHEV and proposed configuration. SHEV: series hybrid electric vehicle.

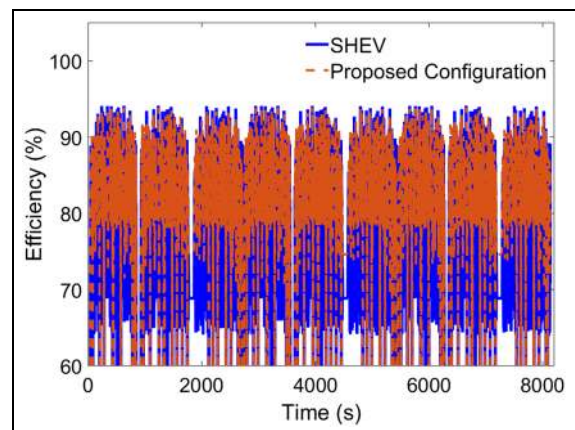


Figure 16. Comparison of efficiency of traction motor for SHEV and proposed configuration. SHEV: series hybrid electric vehicle.

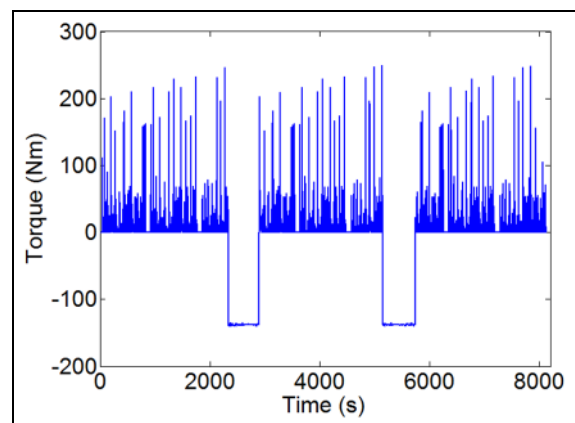


Figure 17. Output torque of the ISG of the proposed configuration. ISG: integrated starter generator.

motor mode assisting the traction motor as long as the battery SOC was within the limit. Negative torque output of the ISG indicated the generator mode of the

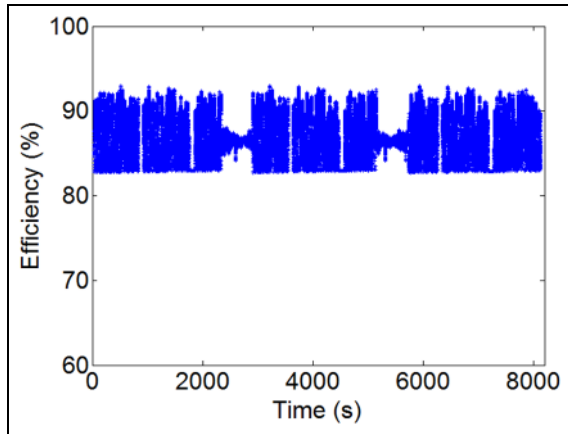


Figure 18. Efficiency curve of the ISG of the proposed configuration.

ISG: integrated starter generator.

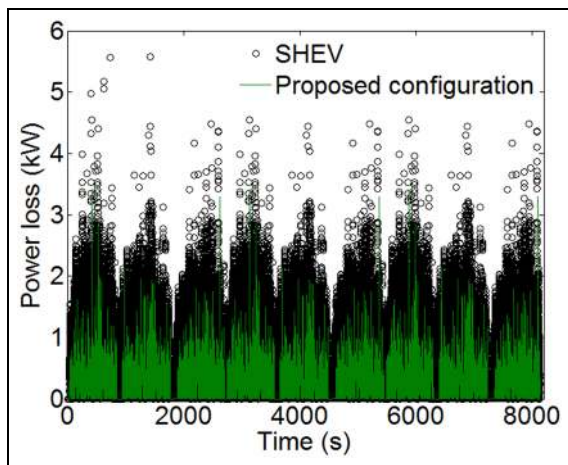


Figure 19. Comparison of the traction motors power loss for SHEV and proposed configuration.

SHEV: series hybrid electric vehicle.

ISG where it provided electric energy to the batteries as the engine was switched on. As the torque requirement is distributed between ISG and the traction motor, the traction motor could be downsized appropriately, which in turn improved the efficiency and the power loss of the electric machine. Figure 18 shows the efficiency of the ISG across the drive cycle. The efficiencies of the motors were assumed constant during initial parameter matching of the vehicle powertrain. However, during simulation of the vehicle powertrain for the on-road IDC in AVL Cruise, the efficiency of the electric machines varied with the load torque to reflect the operating points of the motors. The average efficiency of the traction motor across the on-road IDC was found out to be 78.69%. As the torque requirement is distributed between the ISG and the traction motor, the traction motor could be downsized appropriately, which in turn improved its average efficiency by 10.95% as compared to the traction motor of the

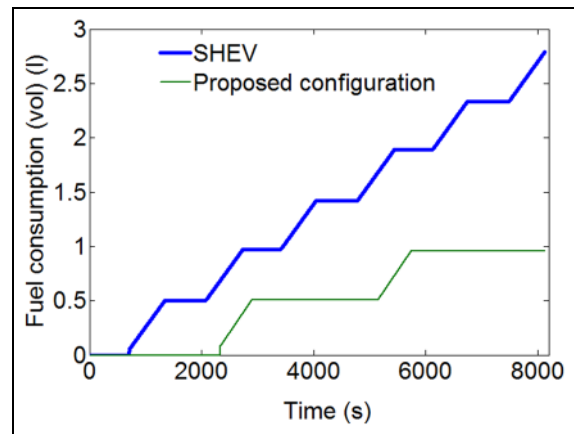


Figure 20. Comparison of fuel consumption for SHEV and the proposed configuration.

SHEV: series hybrid electric vehicle.

SHEV powertrain when simulated for the same drive cycle. A comparison between the power loss of the traction motors of SHEV and the proposed configuration was made in Figure 19. It was observed that the motor power loss for the proposed configuration was lower than the SHEV powertrain by almost 60.26%, when simulated for the on-road IDC (repeated four times).

Operation of engine-generator in the discussed configurations depends on the SOC of the battery and the control strategy. A comparison of the engine performance was made between the SHEV and the proposed configuration for the on-road IDC, in terms of fuel consumption in liters. The cycle has been repeated four times for a better comparison of the vehicle performance. Figure 20 shows that the fuel consumption of the proposed configuration was lower than the SHEV by 61.81%, thereby concluding a better performance of the proposed configuration as compared to the SHEV counterpart.

Analysis of the optimization results

The optimizer developed in this study was run for 500 iterations, where the convergence of the objective and the constraint functions was obtained after the 100th iteration. With this, the optimal objective value in terms of mpgge was determined. The values of the objective function, the design variables, and the constraints are given in Figures 21–23, respectively, where the design variables and constraints were plotted in a normalized scale of $[-1, 1]$. The optimization procedure was able to satisfy the design constraints with the design variables being within their limits.

The comparison of the fuel economy in terms of mpgge showed an improvement in the proposed configuration by 18.63% as compared to SHEV (Table 8). Table 9 gives the comparison of the component parameters before and after optimization. With optimization, downsizing of the engine, traction motor, ISG,

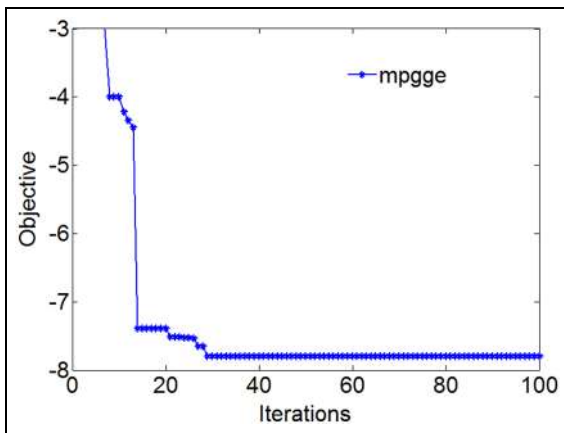


Figure 21. Iterations of the objective function for the proposed configuration.

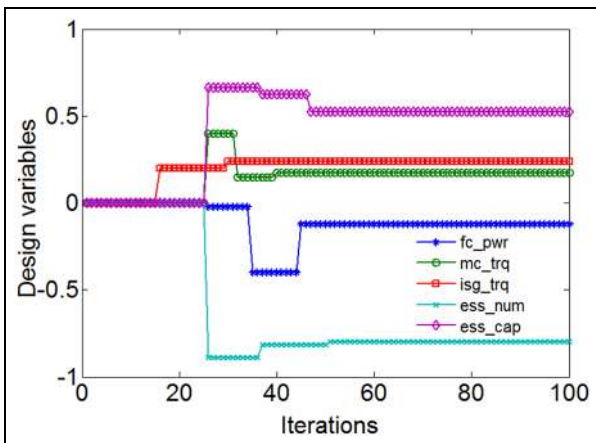


Figure 22. Iterations of the design variables for the proposed configuration.

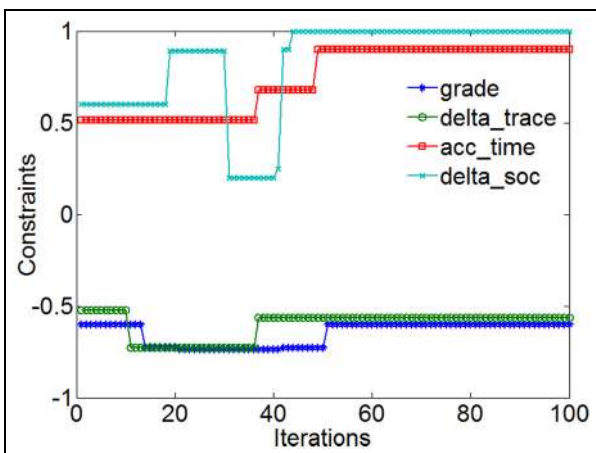


Figure 23. Iterations of the constraints for the proposed configuration.

and the number of battery cells could be achieved. A percentage decrease of 9.53% for engine power could be achieved. Similarly, both the motor power and the ISG power were reduced by 10% and 12.52%, respectively.

Table 8. Comparison of the optimized results.

| Performance parameters | SHEV | Proposed configuration |
|-----------------------------------|------|------------------------|
| mpgge | 5.42 | 6.43 |
| Time (s) to reach 0–50 km/h | 9.2 | 9 |
| Maximum longitudinal speed (km/h) | 98 | 98 |
| Gradeability (%) | 16 | 16 |

mpgge: miles per gallon gasoline equivalent; SHEV: series hybrid electric vehicle.

Table 9. Comparison of the optimized results for the proposed configuration.

| Optimized parameters | Before optimization | After optimization |
|-------------------------|---------------------|--------------------|
| Engine power (kW) | 42 | 38 |
| Motor power (kW) | 135 | 121.50 |
| ISG power (kW) | 54 | 47.24 |
| Number of battery cells | 178 | 170 |
| Battery capacity (Ah) | 70 | 70 |

ISG: integrated starter generator.

Table 10. Comparison of vehicle performance for the proposed configuration.

| Optimized parameters | Before optimization | After optimization |
|-----------------------------|---------------------|--------------------|
| mpgge | 6.43 | 7.8 |
| Time (s) to reach 0–50 km/h | 9 | 8.83 |
| Maximum velocity (km/h) | 98 | 98 |
| Grade (%) | 16 | 16.90 |

mpgge: miles per gallon gasoline equivalent.

The vehicle performance also improved after the optimization of the proposed configuration (Table 10). The fuel economy was improved by 21.31% after optimization as compared to before optimization. The vehicle performance in terms of acceleration, maximum longitudinal speed, and gradeability was met by the optimized proposed configuration.

Figure 24 summarizes the battery SOC history of the powertrains as a function of time for the on-road IDC repeated four times. It could be observed that the charging and discharging cycle of the batteries were less frequent in the proposed configuration as compared to the SHEV, indicating a longer battery life for the proposed powertrain.

Thus, the significant findings of this study could be summarized into two parts as follows:

- Initial parameterization showed an improvement in the performance of the traction motor of the proposed configuration with its operating regions efficiency increased by 10.95% and power loss reduced by 60.26%, when compared to an SHEV. The fuel consumption of the proposed configuration also

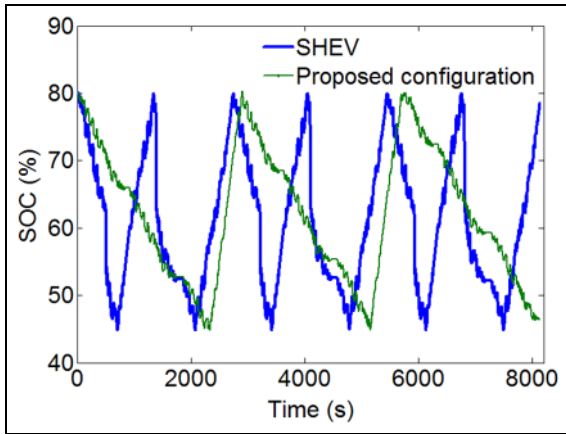


Figure 24. Comparison of SOC history.
SOC: state of charge.

reduced by 61.81% as compared to the SHEV counterpart for an on-road IDC.

- Subsequent optimization of the proposed configuration downsized the ICE, along with a reduction in motor and ISG power by 10% and 12.52%, respectively, when compared to the results before optimization. The optimized proposed configuration also showed an improvement in the vehicle performance with the fuel economy increase by 21.31%, when simulated for an on-road IDC.

Conclusion

This paper developed a modified SHEV powertrain and analyzed its performance with a typical SHEV powertrain for an urban city drive cycle in terms of electric motors' efficiency and fuel economy. The proposed configuration replaced the generator of a typical SHEV with an ISG, that works both as a generator to convert engine power into electricity to charge the batteries and as a motor to drive the wheels, thereby assisting the main traction motor during pure electric driving. The paper presented a methodical development of the HEV powertrain through initial parameter matching based on vehicle dynamics, followed by its optimization to improve the fuel economy and vehicle performance. A rule-based control strategy was developed for the proper operation of the powertrain. The simulation of the proposed configuration and the SHEV for comparative analysis was done for an on-road IDC using the software AVL CRUISE, with the control strategy being implemented in MATLAB/SIMULINK. The following conclusions were made from this study:

- The reduction of GVW of the proposed configuration as compared to SHEV was achieved during initial parameterization of the powertrains. Comparative analysis showed that the GVW of the proposed configuration was reduced by 244 kg (1.5%) as compared to the SHEV powertrain.

- A comparative analysis of the simulation results between the two configurations for an on-road IDC showed an improvement in the working efficiencies of the electric machines, with their operating points in the most efficient regions for the proposed configuration. As the traction motor was downsized during initial parameter matching, the power losses of the traction motor of the proposed configuration were found to be lower than the traction motor of the SHEV powertrain. Simulation results showed that the average efficiency of the traction motor of the proposed configuration improved by 10.95% as compared to the average efficiency of the traction motor of SHEV for the on-road IDC. The average power loss of the traction motor of the proposed configuration was also lower by 60.26% than the traction motor of the SHEV powertrain.
- Optimization results of the proposed configuration showed an improvement in the fuel economy by 21.31% as compared to before optimization for the on-road IDC.
- The fuel consumption of the powertrains was studied by repeating the on-road IDC four times to observe the behavior of the battery SOC and operation of the ICE. The battery SOC was maintained within a lower limit of 0.45 and an upper limit of 0.8 for both configurations. Optimization results showed a lower frequency of charging and discharging of the battery cycle for the proposed configuration as compared to the SHEV, indicating a longer battery life.

Thus, the simulation results, along with the comparison with an SHEV showed the feasibility of the proposed configuration with better vehicle performance and improved fuel economy.

Acknowledgements

The authors thank the Department of Engineering Design, Indian Institute of Technology, Madras, for the necessary support in completing the research work done in this paper. The authors thank AVL CRUISE for providing the license of the software and the support for carrying out the simulations of the powertrain systems. The authors also thank Mr C.S. Nanda Kumar for providing the real-time drive cycle in the city of Coimbatore, India.

Declaration of conflicting interests

The author(s) declared no potential conflicts of interest with respect to the research, authorship, and/or publication of this article.

Funding

The author(s) received no financial support for the research, authorship, and/or publication of this article.

References

1. Department of Heavy Industry, Ministry of Heavy Industries & Public Enterprises, Government of India. National electric mobility mission plan 2020, <http://dhi.nic.in/UserView/index?mid=1347> (accessed September 2016).
2. Mi C, Masrur MA and Gao DW. *Hybrid electric vehicles: principles and applications with practical perspectives*. 1st ed. Hoboken, NJ: Wiley, 2011.
3. Kebriaei M, Sandidzadeh MA, Asaei B, et al. Component sizing and intelligent energy management of a heavy hybrid electric vehicle based on a real drive cycle. *Proc IMechE, Part F: J Rail and Rapid Transit* 2017; 231: 122–132.
4. Shahverdi M, Mazzola MS, Grice Q, et al. Bandwidth-based control strategy for a series HEV with light energy storage system. *IEEE T Veh Technol* 2017; 66: 1040–1052.
5. Yang C, Li L, You S, et al. Cloud computing-based energy optimization control framework for plug-in hybrid electric bus. *Energy* 2017; 125: 11–26.
6. Ehsani M, Gao Y, Gay SE, et al. *Modern electric, hybrid electric and fuel cell vehicles: fundamentals, theory and design*. 2nd ed. Boca Raton, FL: CRC Press, 2005.
7. Yang C, Jiao X, Li L, et al. Robust coordinated control for hybrid electric bus with single-shaft parallel hybrid powertrain. *IET Control Theory A* 2015; 9: 270–282.
8. Li L, Yang C, Zhang Y, et al. Correctional DP-based energy management strategy of plug-in hybrid electric bus for city-bus route. *IEEE T Veh Technol* 2015; 64: 2792–2803.
9. Li X and Williamson SS. Comparative investigation of series and parallel hybrid electric vehicle (HEV) efficiencies based on comprehensive parametric analysis. In: *Proceedings of the IEEE vehicle power and propulsion conference (VPPC 2007)*, Arlington, TX, 9–12 September 2007, pp.499–505. New York: IEEE.
10. Miller MA, Holmes AG, Conlon BM, et al. The GM “Voltec” 4ET50 multi-mode electric transaxle. *SAE Int J Engine* 2011; 4: 1102–1114.
11. Zhu B, Zhang N, Walker P, et al. Two motor two speed power-train system research of pure electric vehicle. SAE technical paper 2013-01-1480, 2013 (SAE world congress and exhibition, 2013, pp.1–5).
12. Wang CL, Yin CL, Luo G, et al. Start and acceleration optimization of a parallel hybrid electric vehicle. *Proc IMechE, Part D: J Automobile Engineering* 2010; 225: 591–607.
13. Viorel IA, Szabo L, Lowenstein L, et al. Integrated starter-generators for automotive applications. *Acta Electrotech* 2004; 45: 255–260.
14. Williamson SS, Wirasingha SG and Emadi A. Comparative investigation of series and parallel hybrid electric drive trains for heavy-duty transit bus applications. In: *Proceedings of the IEEE vehicle power and propulsion conference (VPPC'06)*, Windsor, 6–8 September 2006, pp.1–10. New York: IEEE.
15. Zhou Y, Han C, Wang X, et al. Research on power train source matching for single-axle PHEV. In: *Proceedings of the IEEE vehicle power and propulsion conference (VPPC'08)*, Harbin, China, 3–5 September 2008, pp.1–4. New York: IEEE.
16. Fukuo K, Fujimura A, Saito M, et al. Development of the ultra-low-fuel-consumption hybrid car – INSIGHT (New technologies and new cars). *JSAE Rev* 2001; 22: 95–103.
17. Ehsani M, Rahman KM and Toliyat HA. Propulsion system design of electric and hybrid vehicles. *IEEE T Ind Electron* 1997; 44: 19–27.
18. Gao W and Mi C. Hybrid vehicle design using global optimisation algorithms. *Int J Electr Hybrid Vehicle* 2007; 1: 57–70.
19. Jones DR. DIRECT global optimization algorithm. In: Floudas CA and Pardalos PM (eds) *Encyclopedia of optimization*. Dordrecht: Kluwer Academic Publishers, 2001, pp.431–440.
20. National Renewable Energy Laboratory, Advanced Vehicle Simulator (ADVISOR). Documentation, http://adv-vehicle-sim.sourceforge.net/advisor_doc.html (accessed January 2017).
21. Borthakur S and Subramanian SC. Parameter matching and optimization of a series hybrid electric vehicle powertrain system. In: *Proceedings of the ASME 2016 international mechanical congress and exposition*, Phoenix, AZ, 11–17 November 2016, vol. 12: transportation systems. New York: ASME.
22. Rehman H, Liu N, Xu X, et al. Induction motor drive system for the Visteon integrated starter-alternator. In: *Proceedings of the 25th annual conference of the IEEE industrial electronics society (IECON'99)*, San Jose, CA, 29 November–3 December 1999, vol. 2, pp.636–641. New York: IEEE.
23. Martin GD, Moutoux RD, Myat M, et al. An integrated starter-alternator system using induction machine winding reconfiguration. In: *Proceedings of the IEEE vehicle power and propulsion conference (VPPC 2007)*, Arlington, TX, 9–12 September 2007, pp.677–681. New York: IEEE.
24. Jain AK, Mathapati S, Ranganathan VT, et al. Integrated starter generator for 42-V powernet using induction machine and direct torque control technique. *IEEE T Power Electr* 2006; 21: 701–710.
25. Hughes A and Drury W. *Electric motors and drives: fundamentals, types and applications*. 4th ed. Amsterdam: Elsevier, Ltd, 2013.
26. Erjavec J. *Hybrid, electric and fuel-cell vehicles*. 2nd ed. Clifton Park, NY: Delmar-Cengage Learning, 2013.
27. Chang L. Recent developments of electric vehicles and their propulsion systems. *IEEE Aero El Sys Mag* 1993; 8: 3–6.
28. Nanda Kumar CS. Technical expert, Hybrid vehicle system, India, private communication, 2015.
29. AVL CRUISE-vehicle driveline simulation software, <https://www.avl.com/cruise> (accessed January 2016).

Appendix I

Notation

| | |
|-----------|--|
| a | acceleration in longitudinal direction (m/s ²) |
| \bar{A} | current per meter of the circumference of rotor |
| A_f | frontal cross-section area (m ²) |
| \bar{B} | average of magnitude of flux density (T) |

| | | | |
|----------|---|----------------|--|
| C_d | coefficient of drag | R_f | rolling resistive force (N) |
| C | battery capacity (Ah) | R_g | grade resistance (N) |
| D^2L | rotor volume | T | torque output (N m) |
| E_b | battery energy (W h) | V_b | battery voltage (V) |
| f_r | tire rolling resistance coefficient | W | gross vehicle weight (N) |
| F | required force for acceleration (N) | γ | rotation inertia factor |
| F_t | traction force (N) | η_{isg} | efficiency of the ISG |
| g | acceleration due to gravity (m/s^2) | η_m | efficiency of the motor |
| GVW | gross vehicle weight (kg) | η_t | efficiency of the transmission |
| i_o | transmission ratio | η_g | efficiency of the generator |
| i_{fd} | drive line ratio | η_{bd} | battery discharging efficiency |
| k | torque coupler ratio | θ_s | road gradient angle |
| M | mass of the vehicle (kg) | v_{rm} | vehicle speed corresponding to motor base speed (km/h) |
| P | power (kW) | v_{rv} | vehicle rated speed (km/h) |
| P_b | battery power (kW) | ω_{max} | maximum motor speed (r/min) |
| r | effective wheel radius (m) | | |
| R | total resistance force on the vehicle (N) | | |
| R_a | aerodynamic force (N) | | |